

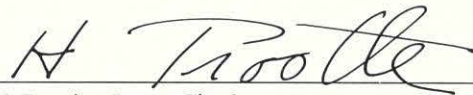
NATIONAL AERONAUTICS AND SPACE ADMINISTRATION  
CONTRACT No. NAS 7-100

*Technical Report No. 32-330*

*Dispersion of  
Long-Period Love Waves in a  
Spherical Earth*

*Robert L. Kovach*

*Don L. Anderson*

A handwritten signature in dark ink, appearing to read 'H. Trostle', is written over a horizontal line.

H. Trostle, Acting Chief  
Research Analysis Section

JET PROPULSION LABORATORY  
CALIFORNIA INSTITUTE OF TECHNOLOGY  
PASADENA, CALIFORNIA

August 30, 1962

Copyright© 1962  
Jet Propulsion Laboratory  
California Institute of Technology

## CONTENTS

I. Introduction . . . . .	1
II. Numerical Calculations and Verification of Results . . . . .	3
III. Earth Models . . . . .	4
IV. Discussion . . . . .	5
V. Displacements . . . . .	6
VI. Conclusions . . . . .	6
Tables . . . . .	7
Figures . . . . .	13
References . . . . .	20

## TABLES

1. Parameters for Gutenberg (1959)-Birch model . . . . .	7
2. Parameters for 8099 models . . . . .	7
3. Parameters for CIT 6 oceanic model . . . . .	8
4. Jeffreys-Bullen A model . . . . .	8
5. Lehmann model . . . . .	9
6. Gutenberg model . . . . .	9
7. Gutenberg (1959)-Birch model . . . . .	10
8. 8099LM model . . . . .	10
9. 8099S model . . . . .	10
10. CIT 6 model . . . . .	11
11. Gutenberg (1959)-Birch model—first higher mode . . . . .	11
12. CIT 6 model—first higher mode . . . . .	11

## FIGURES

1. Shear-wave velocity distributions for continental models . . . . .	13
2. Density distributions for continental and oceanic models . . . . .	14
3. Shear-wave velocity distributions for oceanic models . . . . .	14
4. Love-wave dispersion curves for four continental models compared with recent phase velocity data . . . . .	15
5. Love-wave dispersion curves for three oceanic models compared with recent phase velocity data . . . . .	16
6. Effect of sphericity on Love-wave dispersion for the Jeffreys-Bullen A model . . . . .	17
7. Effect of sphericity on Love-wave dispersion for the CIT 6 model . . .	17
8. Comparison of displacements for continental models computed from flat- and spherical-layer programs . . . . .	18
9. Displacements for CIT 6 model computed using spherical-layer program . . . . .	18
10. Comparison of displacements for CIT 6 model computed from flat- and spherical-layer programs . . . . .	19

## FOREWORD

This Report presents the results of a cooperative research program between the Seismological Laboratory, California Institute of Technology, and this Laboratory. Research at the Seismological Laboratory was carried out under Contract No. NASw-81, sponsored by the National Aeronautics and Space Administration, and Contract No. AF-49(638)910 of the Air Force Office of Scientific Research as part of the Advanced Research Projects Agency's Project VELA.

The authors are grateful to Dr. Russell E. Carr for discussion of various aspects of the theoretical solution, and to Mr. M. Nafi Toksöz and Dr. Ari Ben Menahem for allowing the use of their data in advance of publication.



## ABSTRACT

Periods of torsional eigenvibrations have been computed for heterogeneous spheres corresponding to a variety of Earth models, and the periods of oscillation are used to calculate phase and group velocities for the fundamental and first higher modes of Love waves. A comparison is made between velocities for different spherical models, with the velocities calculated by use of equivalent flat Earth structures. The comparison shows that (1) the effect of sphericity on fundamental-mode Love waves is more complicated than for Rayleigh waves because of the efficient channeling of waves by low-velocity layers, and (2) the first higher Love mode is more affected by curvature than the fundamental mode. The variation with depth of the relative amplitude of the displacements indicates that the first higher Love mode for periods less than 90 sec is very sensitive to upper mantle structure in the vicinity of the low-velocity zone. Comparison of the theoretical results with recent phase-velocity and torsional-oscillation data shows that a Gutenberg-type velocity structure is more satisfactory than either the Lehmann or Jeffreys structures. The use of consistent densities with the Gutenberg model, rather than Bullen A densities, has a small but significant effect on the calculated velocities. For periods greater than 200 sec the calculated phase velocities for various oceanic and continental structures are all within 2% of each other. The calculated group velocities are within  $1\frac{1}{2}\%$  of each other in the range  $150 < T < 400$  sec, thus confirming experimental results. Dispersion measurements must therefore be made to better than this accuracy in order to draw significant conclusions about details of Earth structure.

## I. INTRODUCTION

Many studies, both observational and theoretical, have recently been conducted on the dispersion of long-period Rayleigh waves in the Earth. In an important paper, Dorman, Ewing, and Oliver (Ref. 1) presented extensive computations to explain observed mantle Rayleigh-wave dispersion. Rayleigh-wave dispersion was calculated for

eleven models of continental and oceanic structure for a flat, layered Earth utilizing the Thomson-Haskell matrix formulation. Using data of Ewing and Press (Refs. 2,3), they concluded that the mantle structure under continents proposed by Gutenberg (see Ref. 4) was far superior to the standard Jeffreys-Bullen structure. It was also shown that



a modification of a mantle structure proposed by Lehmann (Ref. 5) was consistent with Pacific Ocean data. Both the Gutenberg and the Lehmann models include a low-velocity zone in the upper mantle. Takeuchi, Press, and Kobayashi (Ref. 6) used a variational method and showed that Rayleigh-wave dispersion data required the existence of Gutenberg's low-velocity zone in the upper mantle. Aki and Press (Ref. 7), using a synthetic seismogram approach, demonstrated that the Atlantic and Indian Oceans also had low-velocity zones and presented an alternate model for the Pacific Ocean.

These fundamental studies all used calculations based on flat Earth models and considered Rayleigh-wave group velocity data in the period range of 50–250 sec. An important question was the influence of gravity and sphericity in this period range. This question was answered by Bolt and Dorman (Ref. 8) and Alterman, Jarosch, and Pekeris (Ref. 9). By numerical integration of the equations of spheroidal motion for four models of a spherical gravitating Earth, Bolt and Dorman concluded that the combined effect of gravity and sphericity on phase velocity could not be ignored for Rayleigh waves with periods greater than about 50 sec, but that group velocities for  $100 < T < 250$  sec were accurate to 1%. The general conclusions of the earlier papers, being based on group velocity data, therefore remained correct. Bolt and Dorman further demonstrated that a Gutenberg velocity structure with Bullen A densities was consistent with phase and group-velocity data out to a 300-sec period.

Alterman, Jarosch, and Pekeris also showed that flat Earth calculations gave phase velocities correct to 1% up to a 50-sec period only, and that group velocities were correct to 1% out to 250 sec. Their solutions for a spherical Earth also favored the Gutenberg mantle structure.

An equivalent study of mantle Love waves has not yet been presented; published results, data, and theory are inconclusive. In a preliminary note Satô, Landisman, and Ewing (Ref. 10) presented theoretical results for Love waves in a spherical Earth with a Jeffreys-Bullen A structure. No comparison was made with data. Takeuchi (Ref. 11); Gilbert and MacDonald (Ref. 12); MacDonald and Ness (Ref. 13); and Pekeris, Alterman, and Jarosch (Ref. 14) also computed theoretical torsional oscillation periods. MacDonald and Ness concluded that a modified Gutenberg mantle fits the torsional oscillation data best, although

the period range considered was not sensitive to details of the upper mantle structure. Kobayashi and Takeuchi (Ref. 15), using flat Earth calculations, concluded that the Jeffrey's model gave better agreement than the Gutenberg model for mantle Love waves. Jobert (Ref. 16) also computed dispersion of Love waves on a spherical Earth for several continental- and oceanic-type structures.

Because a knowledge of Love-wave dispersion gives valuable information concerning the shear-velocity structure in the Earth, extensive calculations are presented here to examine the sensitivity of Love waves to variations in assumed Earth models. The sensitivity of Love waves to variations in internal structure is an important question not only for terrestrial seismology, but also for future planetary exploration.

The method used to obtain the new Love-wave velocities depends on the calculation of the periods of the free torsional modes of vibration for a heterogeneous elastic sphere. An outline of the method was presented by Alterman, Jarosch, and Pekeris (Ref. 17) and is based on earlier analyses by Love (Ref. 18), Hoskins (Ref. 19), and Jeans (Ref. 20). An excellent review of the earlier calculations may be found in Stoneley (Ref. 21). Other techniques used to isolate the torsional eigenvibrations have been the variational method (Jobert, Ref. 22; Takeuchi, Ref. 11), an extension of the Thomson-Haskell matrix method (Gilbert and MacDonald, Ref. 12), and a direct numerical integration of the equations of motion (Satô, Landisman, and Ewing, Ref. 10). Only a limited number of models have been considered in the previous papers and main attention has been focused on the low-order oscillations. There is significant disagreement between many of the published values of vibration periods.

Since any eigenvalue problem requires a large amount of computation time, the results of the calculations are tabulated here in detail. They can be used not only for studying the dispersion of Love waves, but also the free torsional oscillations themselves.

Computations are presented for the fundamental Love mode in the period range from 60 to about 600 sec and are compared with recent phase velocity data. Comparisons are made between flat and spherical calculations for equivalent structures, and the first higher Love mode is investigated for continental and oceanic structures.



## II. NUMERICAL CALCULATIONS AND VERIFICATION OF RESULTS

Alterman, Jarosch, and Pekeris (Ref. 17) have shown that the torsional oscillations can be defined by the system of equations

$$\frac{dy_1}{dx} = \frac{1}{x} y_1 + \frac{a}{\mu(x)} y_2$$

$$\frac{dy_2}{dx} = \left[ \frac{\mu(x)(n^2 + n - 2)}{ax^2} - a\sigma^2 \rho_0(x) \right] y_1 - \frac{3}{x} y_2$$

where

- $a$  = radius of spherical body
- $x$  = normalized radius
- $\mu(x)$  = rigidity
- $\rho_0(x)$  = unperturbed density
- $n$  = order number of spherical harmonic
- $\sigma$  = frequency
- $y_1$  = radial factor of the displacements
- $y_2$  = radial factor of the shear stresses

This system of equations was solved by Carr (Ref. 23) for a solid sphere and coded in Fortran for an IBM 7090 computer. Since this discussion is restricted to oscillations which are confined to the mantle, the presence of a liquid core is of no concern in the immediate problem. However, the boundary conditions are slightly changed for a solid sphere in that regularity at the origin must be satisfied, in addition to the vanishing of stresses at the free surface.

Because the method of solution is thoroughly discussed by Carr, only a brief outline of the numerical solution is given here. The above differential equations are integrated

downward from the free surface using the Adams-Moulton predictor-corrector method. Runge-Kutta-Gill formulas are used to start the integration process and to restart the integration whenever the step size has been changed. The integration step size is variable and is controlled internally by specifying that the truncation error shall not exceed a prescribed bound. Partial double precision is used to control the growth of round-off error. Input data are given in a table of normalized radius, rigidity, and density, and intermediate values needed for computation are obtained internally by referring to the table and interpolating linearly.

Regularity at the origin was met by a power-series expansion for the two dependent variables  $y_1$  and  $y_2$ ; within the radius of convergence of the power series it is required that the solution to the differential equations and the power series match. This requirement gives rise to a characteristic determinant which equals zero for the correct eigenfrequency  $\sigma$ . A sequence of approximations for  $\sigma$  is used, halving the sum of the previous calculations, which makes the characteristic determinant change sign. The process is terminated when the value of  $\sigma$  is unchanged up to a specified number of significant digits.

Verification of the numerical accuracy of the program was accomplished in several ways. The periods of oscillation for  $n = 2, 3$ , and 4 for a homogeneous Moon model were calculated (Carr and Kovach, Ref. 24) and agree exactly with the published values of Takeuchi, Saito, and Kobayashi (Ref. 25) obtained by independent means. Our calculations agree to three significant digits with published values of Satô, Landisman, and Ewing (Ref. 10) for the Jeffreys-Bullen model, and with published values of Pekeris, Alterman, and Jarosch (Ref. 14) for the Gutenberg model.



### III. EARTH MODELS

For the computations presented here the Earth is assumed to consist of spherical shells of variable thickness. Each shell has linear velocity and density gradients. Therefore, any velocity-density distribution can be approximated as closely as is desired by increasing the number of entries in the input tables. Seven models of the Earth's mantle are considered; four models are continental and three, oceanic.

The continental models are the Gutenberg-Bullen A, the Jeffreys-Bullen A, the Lehmann-Bullen A, and the Gutenberg (1959)-Birch models. The Gutenberg-Bullen A model is the same as considered by Pekeris, Alterman and Jarosch. Velocity-density parameters for the Jeffreys-Bullen A and the Lehmann-Bullen A models were taken from Satô, Landisman, and Ewing. The shear velocity and density distributions for the continental models are shown in Figs. 1 and 2.

Because the Gutenberg-Bullen A and the Lehmann-Bullen A models contain inconsistent velocity-density combinations, an additional Earth model, designated the Gutenberg (1959)-Birch model, was constructed. This model is based on the most recent results of compressional and shear velocity obtained by Gutenberg (Ref. 26) and

is characterized by slightly higher shear velocities in the low-velocity zone (Fig. 1) than the familiar Gutenberg model. Density was obtained from the compressional velocity-density relation  $\rho = 1.13 + 0.302V_p$  given by Birch (Ref. 27). This relation is consistent with a mantle of mean atomic weight 22.5 and gives a density reversal in the low-velocity zone (Fig. 2). The variation of the physical parameters for the Gutenberg (1959)-Birch model is given in Table 1. Anderson and Harkrider (Ref. 28) have shown from flat Earth calculations that the difference between Bullen A and Birch densities has only a slight effect on Rayleigh waves and almost negligible effect on Love waves for periods less than 300 sec.

Two of the oceanic models considered are versions of Dorman's model 8099. The model 8099LM (Fig. 3, Table 2) approximates the actual layering used in the flat Earth calculations, while 8099S (Table 2) is constructed with straight-line segments joining layer midpoints. CIT 6 (Table 3) is a smoother structure with a Gutenberg-type low-velocity channel and a Birch-type density structure (Figs. 2, 3). These three similar models allow us to investigate the sensitivity of mantle Love waves to details in the upper mantle.



#### IV. DISCUSSION

Calculated periods and phase velocities are tabulated in Tables 4—12 and shown graphically in Figs. 4 and 5. The data shown in the figures are from recent traveling- and standing-wave analyses. It is apparent from an examination that no one model adequately explains all of the phase velocity data, although it must be remembered that the data are for primarily oceanic paths.

For periods greater than about 200 sec all of the calculated phase velocities are within 2% of each other, but the data do favor a Gutenberg- or Gutenberg-Birch-type mantle structure. It is also interesting to note that, for periods greater than 200 sec, the difference between oceanic and continental models is within the difference between several of the continental models themselves.

All of the oceanic and continental group velocity curves considered are within 1½% of each other within the period range  $150 < T < 400$  sec. This fact implies that group velocity measurements must be made to at least this accuracy in order to differentiate between the various models considered.

Most calculations in the literature have been based on continental-type structures. An oceanic structure is more pertinent if conclusions are to be drawn from free oscillation or world-encircling mantle Love-wave data. Dorman, Ewing, and Oliver (Ref. 1) developed an oceanic model, designated 8099, which they considered a satisfactory solution based on plane layer calculations. Case 8099 is not a completely satisfactory solution in the light of more-recent Rayleigh-wave phase velocity data and spherical Earth solutions, but it serves as a convenient reference case. Furthermore, the densities used in 8099 are derived from Jeffrey's velocities and are therefore inconsistent with the actual velocity structure used. The two versions of 8099 considered here are shown in Fig. 3 and tabulated in Table 2. Aside from being two possible oceanic structures, these cases may be considered two extreme methods for approximating the same smooth structure. As shown in Fig. 5, the two structures give quite different dispersion.

CIT 6 is a smooth structure with a low-velocity channel and a consistent density. The phase velocity curve for this model falls between 8099S and 8099LM, although all three curves fall generally within the scatter of the data. The recent data of Toksöz and Ben Menahem (personal

communication) favors CIT 6 in the period range from 60 to about 170 sec. Between 200 and 350 sec the data favor 8099 LM, and beyond 400 sec either CIT 6 or 8099 LM are satisfactory, although the data scatter. It is noted that for these long periods the continental Gutenberg structures are equally satisfactory as the above-mentioned oceanic structures.

Since many previous calculations have been based on plane layered models of the Earth, it is important to know how sphericity affects these results. Flat Earth equivalents have been computed for the Jeffreys-Bullen A and CIT 6 structures. The resulting dispersion is shown in Figs. 6 and 7. The Jeffreys-Bullen A model behaves as expected, with the flat and spherical solutions converging at short periods.

For this model an approximate empirical relation between phase velocities in a spherical and a plane layered halfspace can be determined

$$c \approx c_h + 0.00016T$$

valid to within 0.5% in the period range  $100 < T < 350$  sec. This correction is good for the Jeffreys-Bullen A model and presumably for similar Earth models. Group velocities for this model computed using flat or spherical layers agree to 1% in the period range 140–350 sec.

A comparison between flat and spherical calculations for CIT 6 gives a somewhat more surprising result. Instead of converging, the two phase velocity curves are almost parallel, the spherical case having phase velocities about 0.065 km/sec higher than the equivalent flat case in the period range  $70 < T < 300$  sec. This can be shown to be due to the presence of the low-velocity channel which, for SH motion, acts as an efficient energy trap. In a certain period range the fundamental-mode Love wave is as much a channel mode as a surface mode and is therefore traveling around a smaller sphere.

As can be seen in Fig. 5, the effect of sphericity on the first higher Love mode is large. Use of fundamental and higher mode Love-wave data to determine Earth structure apparently must include the effect of sphericity, even for periods as short as 20 sec. However, this situation improves if it can be demonstrated that no low-velocity zone exists in the depth interval of interest.



## V. DISPLACEMENTS

The variation of displacements and stresses with depth are calculated routinely in the process of finding the eigenfrequencies. Displacements and stresses are important not only for checking convergence and verifying mode number, but also for determining energies and the resulting effect on dispersion of various sections of the spherical wave guide.

The displacements for two-period ranges for two continental models are shown in Fig. 8. The Gutenberg-Birch and the Jeffreys-Bullen A model give quite different dispersion, but the displacements with depth are similar. Displacements for an equivalent flat Earth model are greater for the fundamental mode and show that Love waves over a spherical Earth sample less deep than on an equivalent flat Earth.

Normalized displacements in the fundamental and first higher Love modes are shown in Fig. 9 for the CIT 6 model. The higher modes of a given order number sample successively deeper. Since the higher modes sample the mantle differently than the fundamental mode, the use of higher-mode data promises to be important in determining a unique structure.

Comparison between displacements in a spherical Earth and in a flat Earth are made in Fig. 10 for both the fundamental and first higher Love mode. The effect of sphericity is to migrate the displacements away from the center of curvature of the displacement-depth function. As is evident from the dispersion (Fig. 7) and the variation of displacements with depth, sphericity has a larger effect on higher-mode Love waves than on the fundamental mode.

## VI. CONCLUSIONS

In addition to providing theoretical results for mantle Love waves for seven models of a heterogeneous spherical Earth, several important conclusions can be drawn from this analysis.

- (1) For the models considered here, the effect of sphericity on fundamental-mode Love waves of periods greater than some 200 sec is less extreme, although more complicated, than on Rayleigh waves. A low-velocity channel seems to be more effective in trapping energy for Love waves and, therefore, makes the effect of sphericity show up at very short periods. The sphericity correction is a strong function of Earth structure.
- (2) Displacement-with-depth calculations indicate that the first higher Love mode for periods less than 90 sec is very sensitive to the upper mantle structure in the vicinity of the low-velocity zone and is a potentially useful source of information for analyzing the details of this region.
- (3) The data seem to favor a CIT 6 oceanic upper mantle structure and a Gutenberg or Gutenberg-Birch lower mantle structure. However, it is preferable to use a Gutenberg-Birch structure because of the consistent velocity-density relation.
- (4) For periods greater than 200 sec the difference between the dispersion for oceanic and continental structures is no greater than the difference between the dispersion for various proposed continental models themselves.
- (5) The group velocity of mantle Love waves is much less sensitive to different structures than is the phase velocity.
- (6) More precise and consistent experimental Love-wave dispersion data are needed before the question of the best model for the Earth's mantle can be resolved.



Table 1. Parameters for Gutenberg (1959)-Birch model

$R/R_0^a$	$\beta$ km/sec	$\rho$ g/cm <sup>3</sup>	$\mu \times 10^{11}$ dyne/cm <sup>2</sup>
1.0000	3.55	2.84	3.579
0.9940	3.55	2.84	3.579
0.9940	4.60	3.57	7.554
0.9906	4.51	3.507	7.133
0.9874	4.45	3.486	6.903
0.9843	4.42	3.495	6.828
0.9812	4.40	3.513	6.801
0.9780	4.39	3.528	6.799
0.9749	4.40	3.546	6.865
0.9717	4.42	3.564	6.963
0.9686	4.45	3.582	7.093
0.9655	4.48	3.606	7.237
0.9623	4.52	3.628	7.412
0.9592	4.565	3.652	7.610
0.9561	4.61	3.676	7.812
0.9529	4.66	3.700	8.035
0.9451	4.81	3.773	8.729
0.9372	4.95	3.848	9.429
0.9294	5.09	3.924	10.166
0.9215	5.22	3.996	10.888
0.9137	5.36	4.071	11.696
0.9058	5.50	4.147	12.545
0.8901	5.77	4.301	14.319
0.8744	6.04	4.422	16.132
0.8587	6.30	4.543	18.031
0.8430	6.35	4.573	18.439
0.8116	6.50	4.694	19.832
0.7803	6.60	4.769	20.774
0.7489	6.75	4.845	22.075
0.7175	6.85	4.920	23.086
0.6861	6.95	4.996	24.132
0.6547	7.00	5.056	24.774
0.6233	7.10	5.116	25.790
0.5919	7.20	5.192	26.915
0.5605	7.25	5.267	27.685
0.5448	7.20	5.267	27.304
0.5417	7.20	5.252	27.226

<sup>a</sup>  $R_0 = 6371$  km

Table 2. Parameters for 8099 models

$R/R_0^a$		$\beta$	$\rho$	$\mu \times 10^{11}$
8099LM	8099S	km/sec	g/cm <sup>3</sup>	dyne/cm <sup>2</sup>
1.0000	1.0000	1.000	1.030	0.103
0.9990	0.9990	1.000	2.100	0.210
0.9980	0.9987	3.700	2.840	3.888
0.9970	0.9944	4.613	3.340	7.106
0.9910		4.613	3.340	7.106
0.9900	0.9780	4.300	3.443	6.365
0.9655		4.300	3.443	6.365
0.9640	0.9576	4.600	3.527	7.462
0.9500		4.600	3.527	7.462
0.9480	0.9427	4.800	3.604	8.304
0.9356		4.800	3.604	8.304
0.9286	0.9286	5.193	3.765	10.152
0.9137	0.9137	5.492	4.010	12.097
	0.8980	5.790	4.230	14.181
	0.8823	6.030	4.410	16.035
	0.8666	6.200	4.545	17.471
	0.8509	6.315	4.640	18.504
	0.8352	6.400	4.710	19.292
	0.8195	6.465	4.770	19.937
	0.8038	6.531	4.828	20.593
	0.7881	6.591	4.883	21.209
	0.7724	6.650	4.940	21.846
	0.7567	6.704	5.000	22.472
	0.7410	6.755	5.055	23.066
	0.7253	6.802	5.105	23.617
	0.7096	6.852	5.158	24.212
	0.6939	6.897	5.208	24.769
	0.6782	6.945	5.265	25.397

<sup>a</sup>  $R_0 = 6371$  km

Table 3. Parameters for CIT 6 oceanic model

$R/R_0^a$	$\beta$ km/sec	$\rho$ g/cm <sup>3</sup>	$\mu \times 10^{11}$ dyne/cm <sup>2</sup>
1.0000	1.000	1.000	0.100
0.9996	1.000	1.000	0.100
0.9991	1.000	2.100	0.210
0.9987	3.700	2.840	3.888
0.9976	4.600	3.535	7.480
0.9965	4.612	3.555	7.560
0.9957	4.612	3.555	7.560
0.9945	4.609	3.550	7.540
0.9922	4.560	3.520	7.320
0.9890	4.450	3.470	6.870
0.9859	4.339	3.420	6.440
0.9827	4.300	3.400	6.287
0.9796	4.290	3.390	6.240
0.9765	4.290	3.390	6.240
0.9733	4.301	3.400	6.290
0.9702	4.322	3.410	6.370
0.9670	4.360	3.462	6.581
0.9639	4.402	3.515	6.810
0.9608	4.460	3.585	7.130
0.9576	4.521	3.625	7.410
0.9513	4.661	3.720	8.080
0.9482	4.741	3.760	8.450
0.9451	4.824	3.790	8.820
0.9403	4.911	3.830	9.238
0.9333	5.040	3.890	9.880
0.9254	5.210	3.950	10.722
0.9137	5.450	4.010	11.910
0.8980	5.761	4.210	13.970
0.8823	6.030	4.400	16.000
0.8666	6.230	4.560	17.700
0.8509	6.322	4.630	18.504
0.8273	6.421	4.740	19.540
0.7959	6.550	4.850	20.810
0.7645	6.690	4.960	22.200
0.7332	6.780	5.070	23.306
0.7018	6.900	5.190	24.710
0.6704	6.97	5.290	25.70
0.6390	7.05	5.390	26.79
0.6076	7.15	5.490	28.07
0.5762	7.23	5.590	29.22
0.5528	7.20	5.690	29.50

<sup>a</sup> $R_0 = 6371$  km

Table 4. Jeffreys-Bullen A model

Order $n$	$T$ sec	$c$ km/sec
18	386.67	5.595
20	355.60	5.490
22	329.42	5.400
24	307.01	5.321
25	296.96	5.286
26	287.57	5.252
28	270.53	5.191
30	255.46	5.137
32	242.02	5.088
34	229.96	5.045
36	219.07	5.005
38	209.19	4.970
40	200.18	4.937
42	191.93	4.907
44	184.34	4.879
46	177.34	4.853
48	170.87	4.830
50	164.86	4.807
52	159.27	4.787
54	154.05	4.767
56	149.17	4.749
58	144.60	4.731
60	140.31	4.715
62	136.27	4.699
64	132.46	4.684
66	128.87	4.670
68	125.47	4.657
70	122.25	4.644
72	119.23	4.630
74	116.33	4.618
76	113.58	4.607

Table 5. Lehmann model

Order <i>n</i>	<i>T</i> sec	<i>c</i> km/sec
18	386.81	5.593
20	355.67	5.489
22	329.44	5.400
24	306.97	5.322
25	296.89	5.287
26	287.48	5.254
28	270.39	5.194
30	255.27	5.141
32	241.78	5.093
34	229.68	5.051
36	218.74	5.013
38	208.82	4.978
40	199.77	4.947
42	191.47	4.918
44	183.85	4.892
46	176.82	4.868
48	170.31	4.846
50	164.26	4.825
52	158.64	4.806
54	153.39	4.788
58	143.87	4.755
60	139.55	4.741
62	135.48	4.727
64	131.65	4.714
66	128.02	4.701
68	124.60	4.689
70	121.35	4.678
72	118.27	4.668
74	115.35	4.657
76	112.57	4.648
78	109.92	4.639
80	107.40	4.630
84	102.58	4.618

Table 6. Gutenberg model

Order <i>n</i>	<i>T</i> sec	<i>c</i> km/sec
18	391.18	5.531
20	359.91	5.426
22	333.52	5.334
24	310.89	5.256
25	300.74	5.220
26	291.24	5.187
28	274.00	5.126
30	258.73	5.073
32	245.09	5.025
34	232.85	4.983
36	221.78	4.945
38	211.73	4.910
40	202.56	4.880
42	194.15	4.851
44	186.42	4.826
46	179.28	4.802
48	172.67	4.780
50	166.53	4.760
52	160.82	4.741
54	155.49	4.724
56	150.50	4.708
58	145.82	4.693
60	141.43	4.679
62	137.29	4.665
64	133.39	4.653
66	129.70	4.641
68	126.22	4.630
70	122.92	4.619
72	119.79	4.609
74	116.81	4.600
76	113.98	4.591
78	111.29	4.582
80	108.72	4.574



Table 7. Gutenberg (1959)-Birch model

Order <i>n</i>	<i>T</i> sec	<i>c</i> km/sec
18	393.10	5.505
20	361.29	5.405
22	334.48	5.319
24	311.54	5.245
26	291.65	5.179
28	274.23	5.122
30	258.82	5.071
32	245.09	5.025
34	232.78	4.985
36	221.66	4.948
38	211.58	4.914
40	202.39	4.884
42	193.98	4.856
44	186.24	4.830
46	179.11	4.806
48	172.51	4.784
50	166.39	4.764
52	160.70	4.745
54	155.38	4.727
56	150.41	4.710
58	145.76	4.695
60	141.38	4.680
62	137.27	4.666
64	133.39	4.653
66	129.73	4.640
68	126.27	4.628
70	122.99	4.617
72	119.88	4.606
74	116.92	4.596
76	114.11	4.586
78	111.43	4.576
80	108.88	4.567
82	106.45	4.558
84	104.13	4.550
86	101.90	4.541
88	99.77	4.534
90	97.73	4.526

Table 8. 8099LM model

Order <i>n</i>	<i>T</i> sec	<i>c</i> km/sec
16	429.06	5.654
18	391.30	5.529
20	359.95	5.424
22	333.59	5.332
24	311.01	5.253
25	300.85	5.217
26	291.35	5.184
28	274.09	5.124
30	258.81	5.070
32	245.17	5.023
34	232.91	4.981
36	221.83	4.943
38	211.76	4.909
40	202.57	4.879
42	194.15	4.851
44	186.40	4.825
46	179.25	4.802
48	172.63	4.780
50	166.48	4.761
52	160.75	4.742
54	155.41	4.726
56	150.41	4.710
58	145.72	4.695

Table 9. 8099S model

Order <i>n</i>	<i>T</i> sec	<i>c</i> km/sec
14	472.75	5.839
16	425.83	5.696
18	388.08	5.575
20	356.85	5.471
22	330.47	5.383
25	297.85	5.270
26	288.39	5.237
27	279.54	5.207
28	271.21	5.178
29	263.39	5.151
30	255.99	5.126
31	249.00	5.103
32	242.41	5.080
33	236.18	5.059
34	230.27	5.038
35	224.64	5.019
36	219.28	5.001
37	214.17	4.984
38	209.29	4.967
39	204.63	4.952
40	200.18	4.937
50	164.41	4.821
60	139.49	4.743
75	113.65	4.664
80	107.04	4.645
90	95.89	4.612

Table 10. CIT 6 model

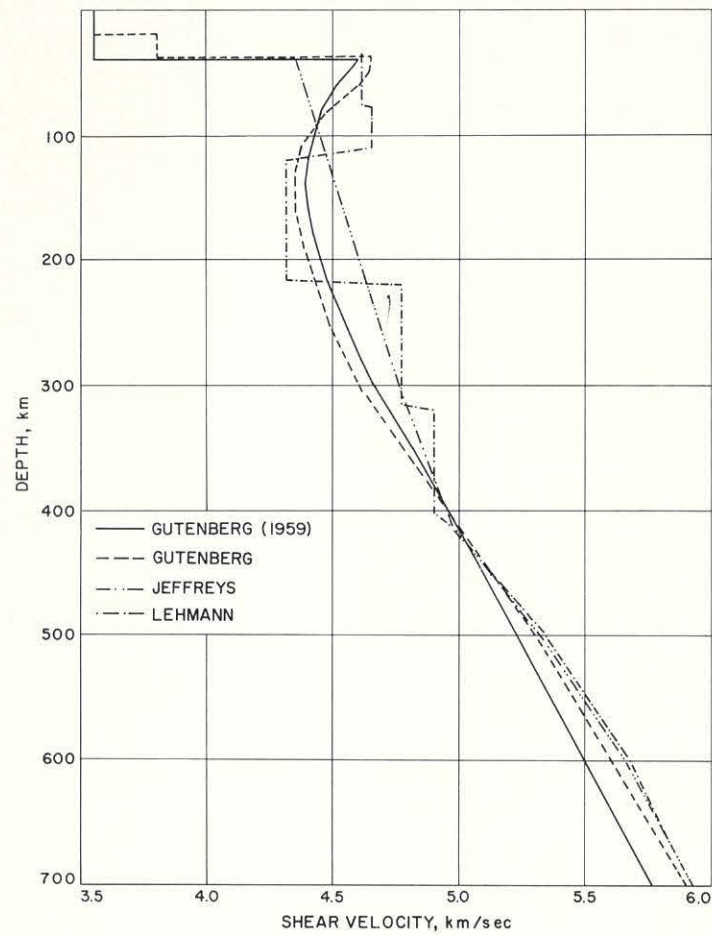
Order <i>n</i>	<i>T</i> sec	<i>c</i> km/sec
14	475.62	5.804
16	428.42	5.662
18	390.38	5.542
20	358.93	5.440
22	332.39	5.352
24	309.69	5.275
26	289.97	5.209
28	272.68	5.150
30	257.37	5.099
32	243.72	5.053
34	231.46	5.012
35	225.78	4.993
36	220.38	4.976
38	210.33	4.943
40	201.16	4.913
42	192.75	4.886
44	185.03	4.861
46	177.89	4.839
48	171.29	4.818
50	165.16	4.799
52	159.45	4.781
54	154.13	4.765
56	149.15	4.750
58	144.47	4.736
60	140.09	4.723
62	135.95	4.710
63	133.98	4.704
64	132.06	4.699
66	128.38	4.688
79	108.68	4.632
80	107.41	4.629
82	104.96	4.622
84	102.62	4.616
86	100.38	4.610
88	98.24	4.604
90	96.18	4.598
92	94.21	4.593
94	92.31	4.588
96	90.50	4.583
98	88.75	4.579
99	87.90	4.576
100	87.06	4.574
102	85.44	4.570
110	79.5	4.55
112	78.2	4.55
120	73.2	4.54
130	67.8	4.53

Table 11. Gutenberg (1959)-Birch model—  
first higher mode

Order <i>n</i>	<i>T</i> sec	<i>c</i> km/sec
72	95.44	5.785
74	93.44	5.751
76	91.53	5.717
78	89.70	5.685
80	87.94	5.655
82	86.25	5.625
84	84.64	5.597
86	83.08	5.570
88	81.59	5.544
90	80.15	5.519

Table 12. CIT 6 model—first higher mode

Order <i>n</i>	<i>T</i> sec	<i>c</i> km/sec
36	158.39	6.923
38	152.40	6.821
40	146.91	6.727
50	125.04	6.338
52	121.50	6.274
54	118.18	6.214
56	115.04	6.158
58	112.09	6.104
60	109.29	6.053
62	106.63	6.006
64	104.11	5.960
66	101.72	5.917
67	100.56	5.896
68	99.44	5.876
72	95.18	5.800
74	93.20	5.765
76	91.30	5.731
80	87.73	5.667
90	79.96	5.531
92	78.58	5.507
100	73.51	5.418



**Fig. 1. Shear-wave velocity distributions for continental models**



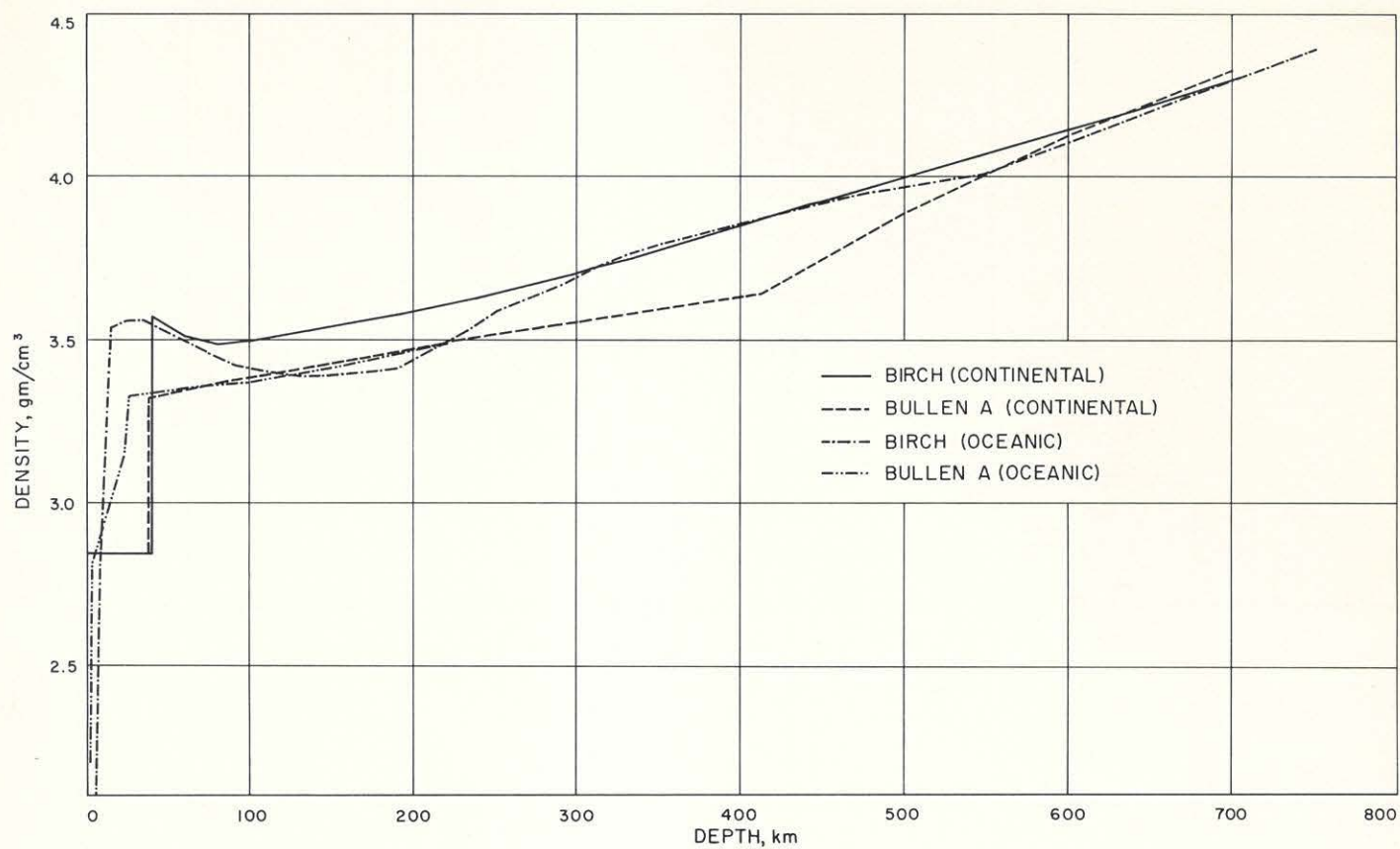


Fig. 2. Density distributions for continental and oceanic models

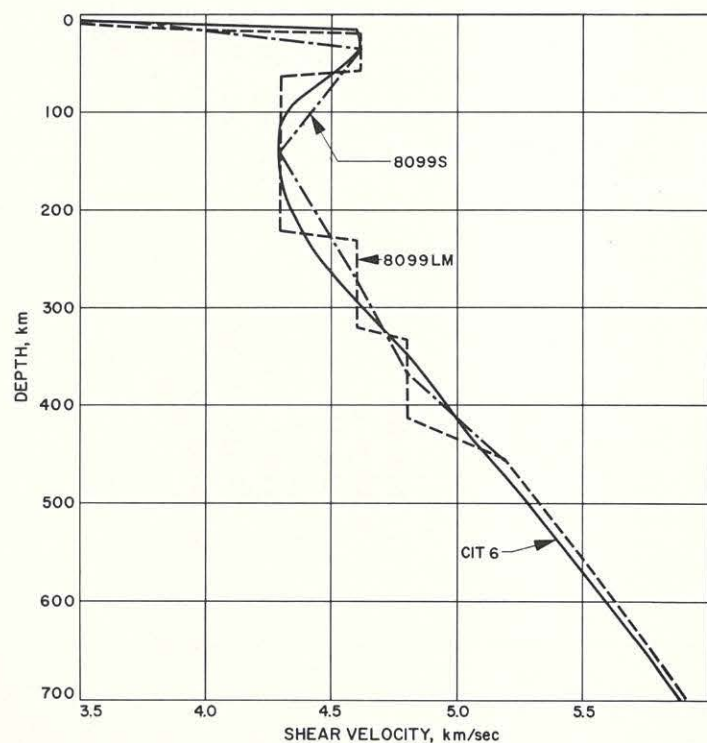


Fig. 3. Shear-wave velocity distributions for oceanic models

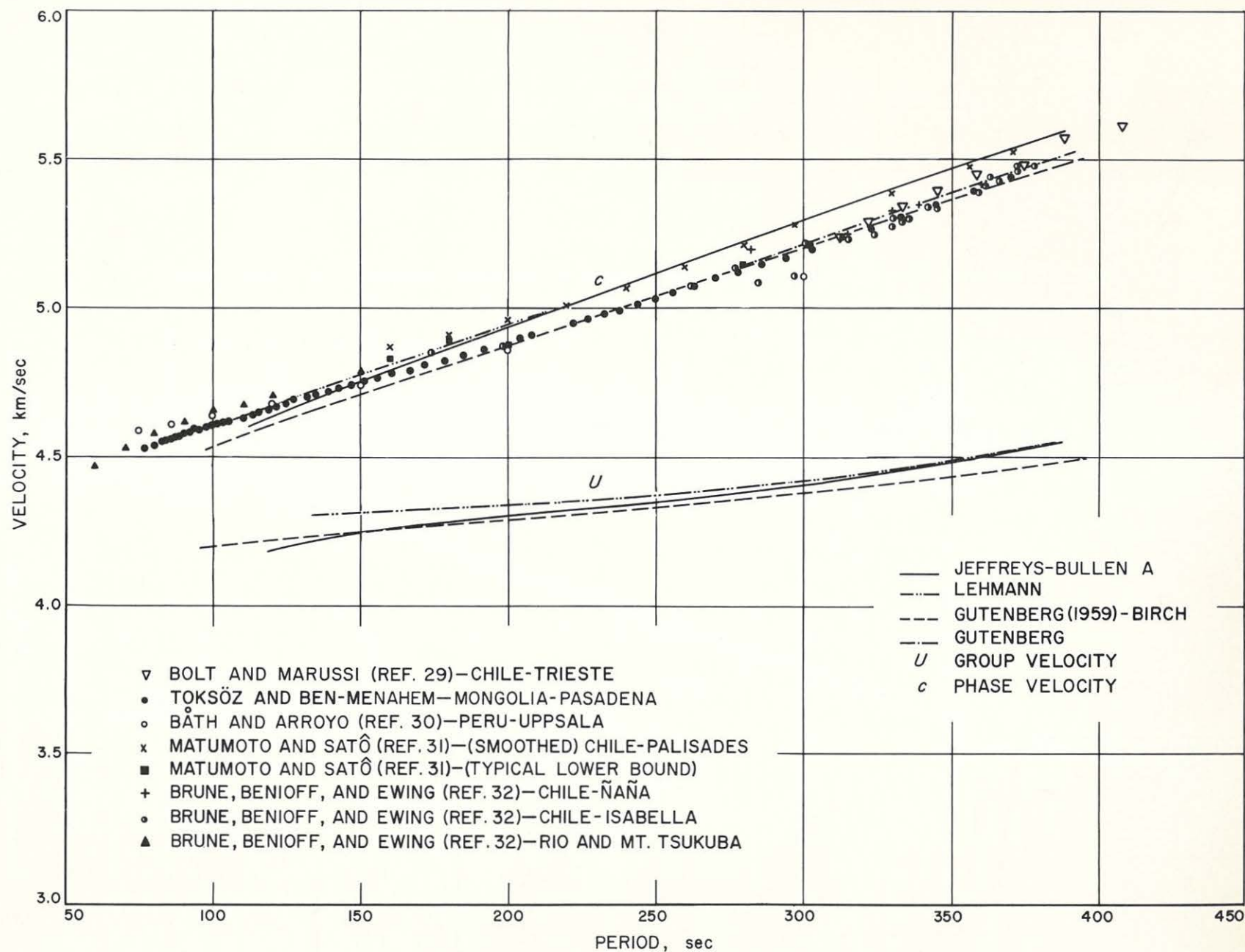


Fig. 4. Love-wave dispersion curves for four continental models compared with recent phase velocity data.

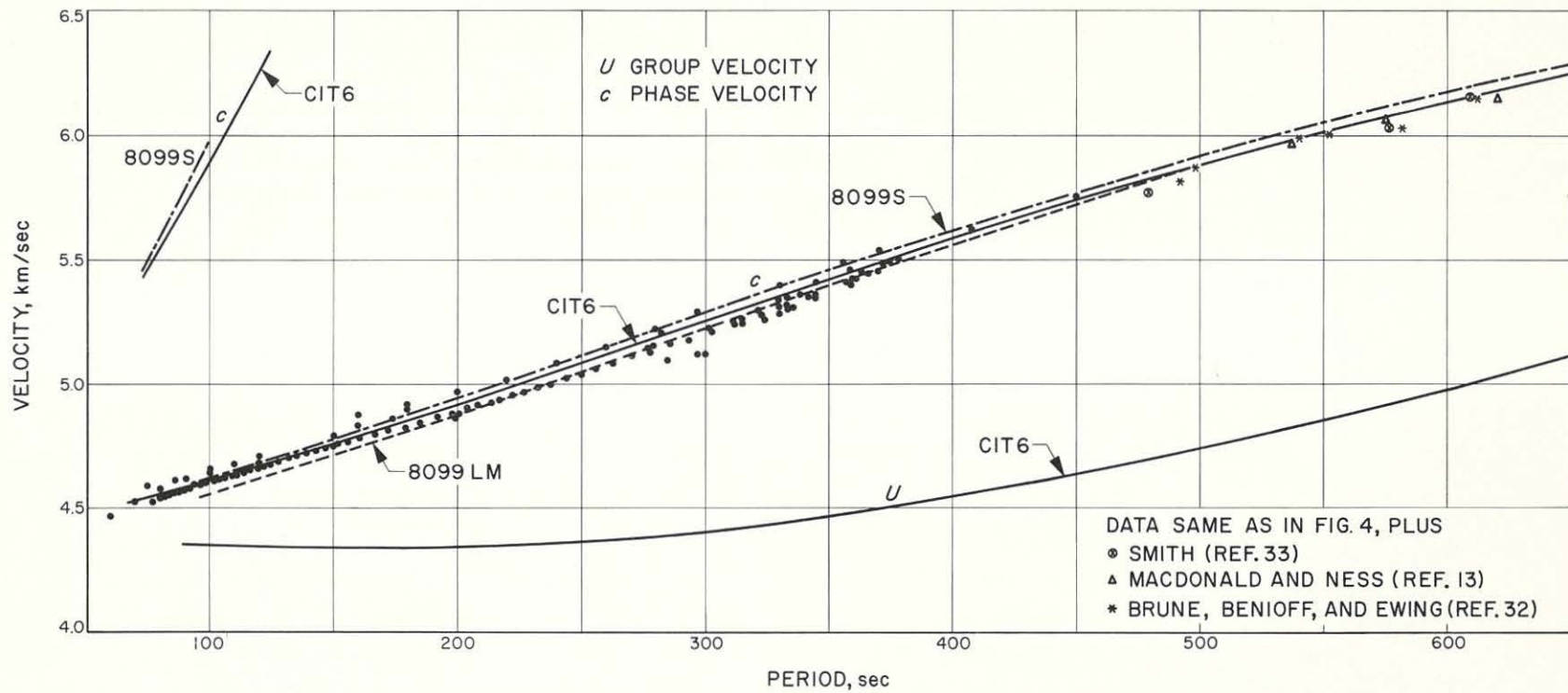


Fig. 5. Love-wave dispersion curves for three oceanic models compared with recent phase velocity data



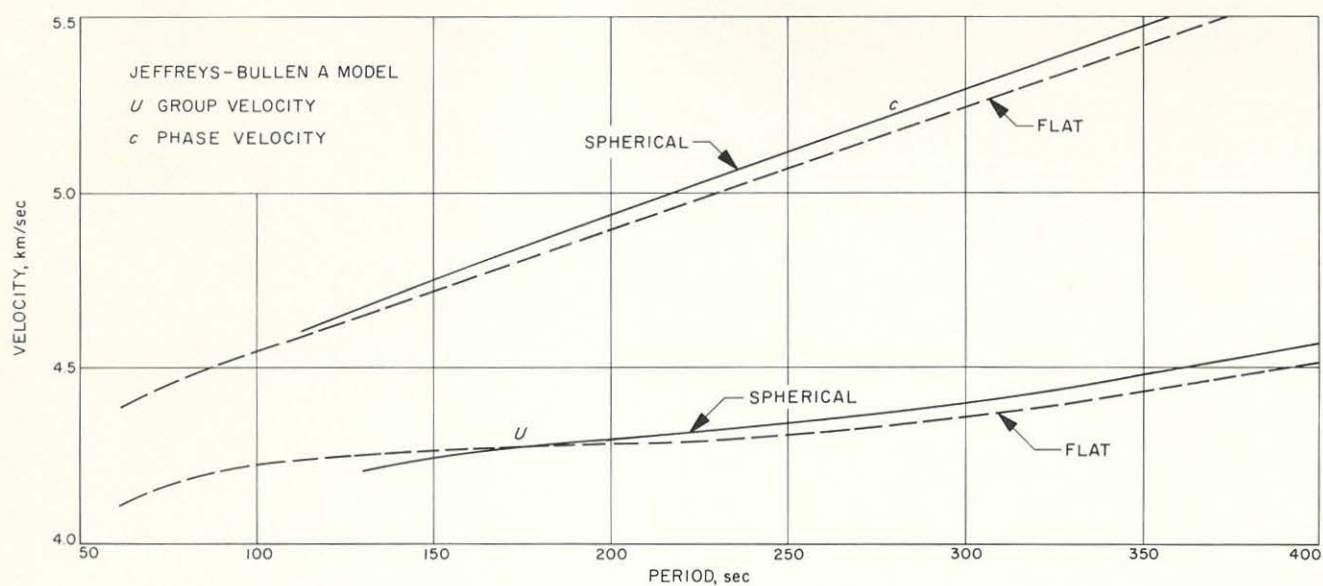


Fig. 6. Effect of sphericity on Love-wave dispersion for the Jeffreys-Bullen A model

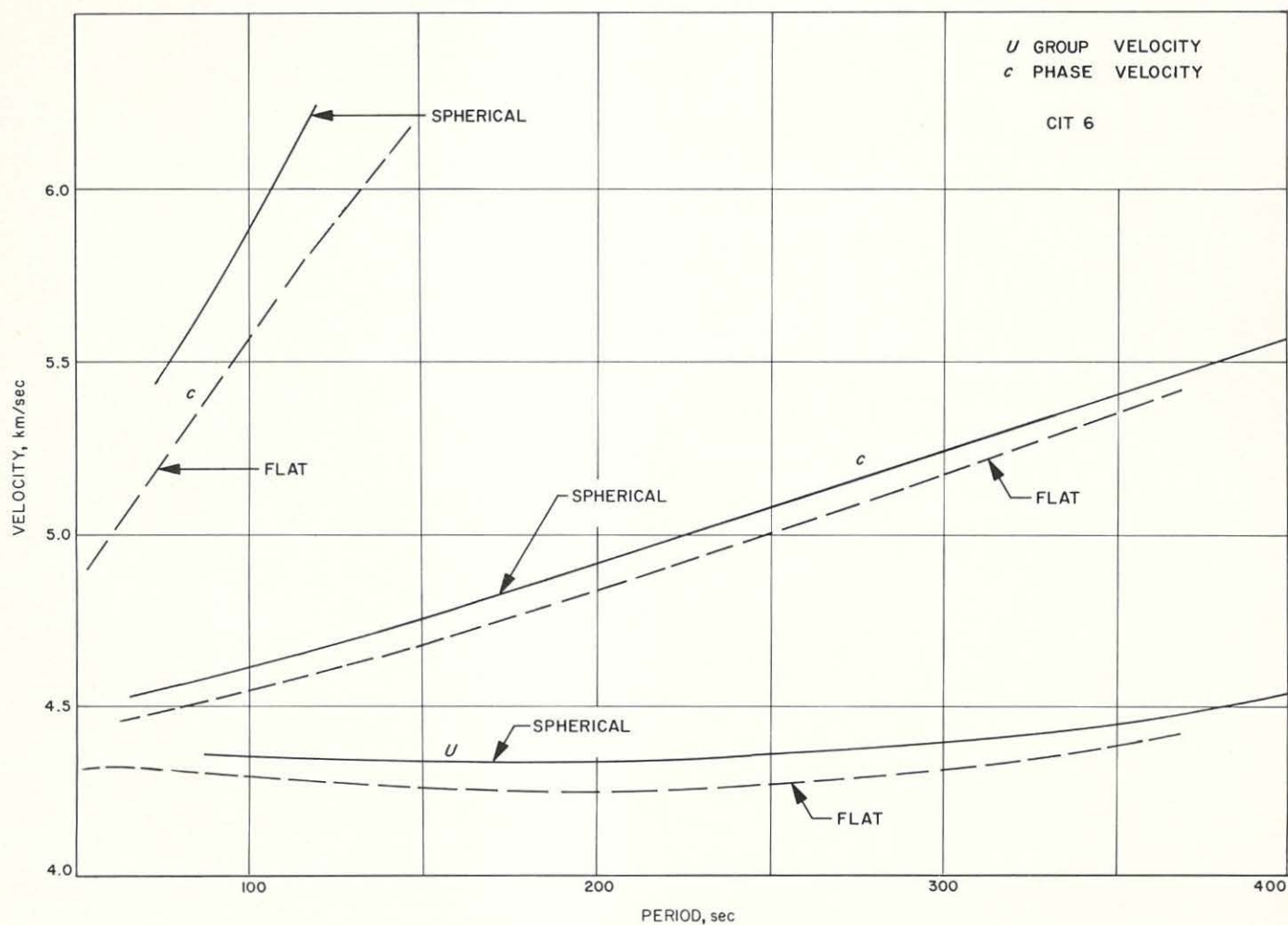


Fig. 7. Effect of sphericity on Love-wave dispersion for the CIT 6 model

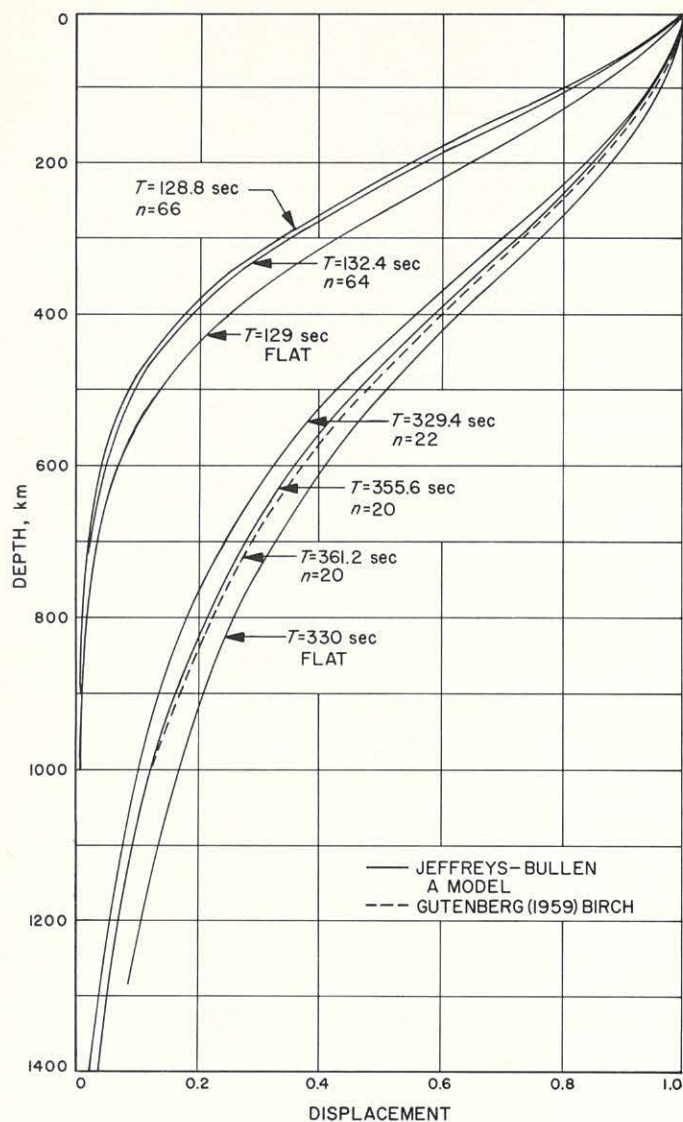


Fig. 8. Comparison of displacements for continental models computed from flat- and spherical-layer programs

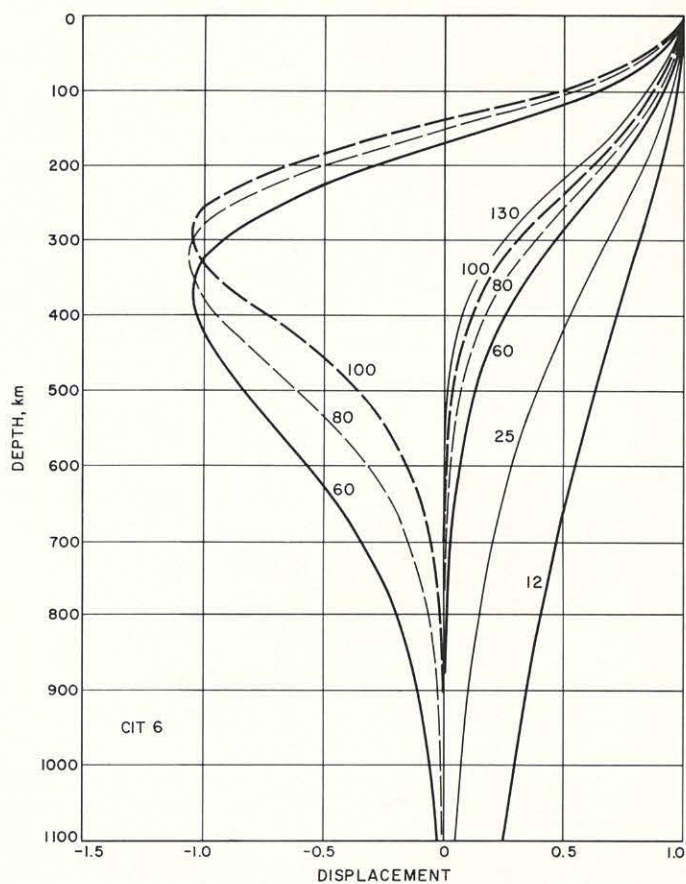


Fig. 9. Displacements for CIT 6 model computed using spherical-layer program



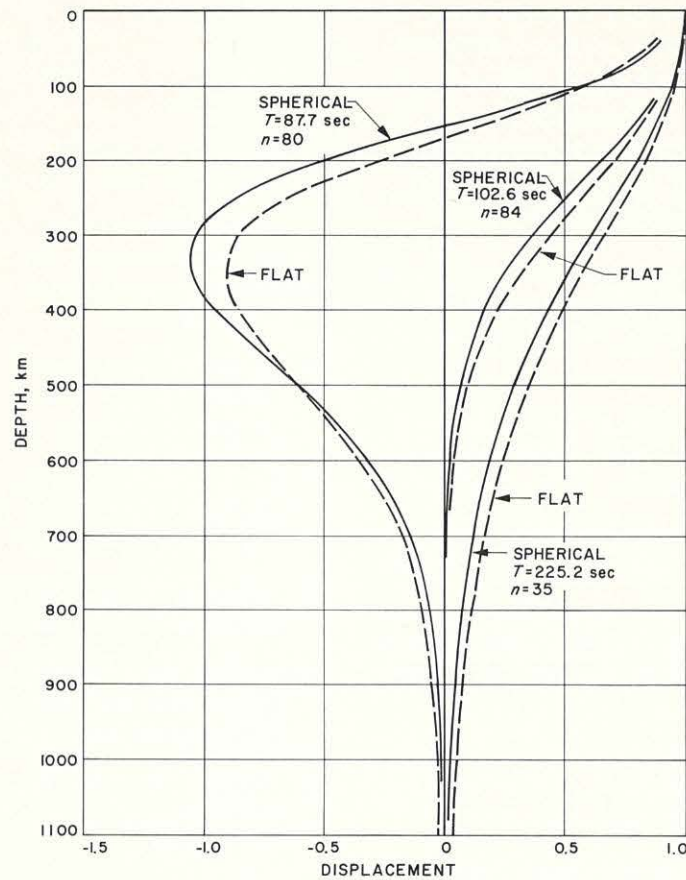


Fig. 10. Comparison of displacements for CIT 6 model computed from flat- and spherical-layer programs

## REFERENCES

1. Dorman, J., M. Ewing, and J. Oliver, "Study of Shear Velocity Distribution by Mantle Rayleigh Waves," *Bulletin of the Seismological Society of America*, Vol. 50, pp. 87-115, 1960.
2. Ewing, M., and F. Press, "An Investigation of Mantle Rayleigh Waves," *Bulletin of the Seismological Society of America*, Vol. 44, pp. 127-148, 1954a.
3. Ewing, M., and F. Press, "Mantle Rayleigh Waves From the Kamchatka Earthquake of November 4, 1952," *Bulletin of the Seismological Society of America*, Vol. 44, pp. 471-479, 1954b.
4. Bullard, E. C., "The Density Within the Earth," *Verhandeling van het Nederlands Geologisch-Mijnbouwkundig, Genootschap, Geologische Serie*, Vol. 18, pp. 23-41, 1957.
5. Lehmann, I., "The Times of P and S in Northeastern America," *Annali di Geofisica* (Rome), Vol. 8, pp. 351-370, 1955.
6. Takeuchi, H., F. Press, and N. Kobayashi, "Rayleigh Wave Evidence for the Low Velocity Zone in the Mantle," *Bulletin of the Seismological Society of America*, Vol. 49, pp. 355-364, 1959.
7. Aki, K., and F. Press, "Upper Mantle Structure Under Oceans and Continents From Rayleigh Waves," *Geophysical Journal*, Vol. 5, pp. 292-305, 1961.
8. Bolt, B., and J. Dorman, "Phase and Group Velocities of Rayleigh Waves in a Spherical, Gravitating Earth," *Journal of Geophysical Research*, Vol. 66, pp. 2965-2981, 1961.
9. Alterman, Z., H. Jarosch, and C. L. Pekeris, "Propagation of Rayleigh Waves in the Earth," *Geophysical Journal*, Vol. 4, pp. 219-241, 1961.
10. Satô, Y., M. Landisman, and M. Ewing, "Love Waves in a Heterogeneous, Spherical Earth," *Journal of Geophysical Research*, Vol. 65, pp. 2395-2404, 1960.
11. Takeuchi, H., "Torsional Oscillations of the Earth and Some Related Problems," *Geophysical Journal*, Vol. 2, pp. 89-100, 1959.
12. Gilbert, F., and G. J. F. MacDonald, "Free Oscillations of the Earth, 1, Toroidal Oscillations," *Journal of Geophysical Research*, Vol. 65, pp. 675-693, 1960.
13. MacDonald, G. J. F., and N. F. Ness, "A Study of the Free Oscillations of the Earth," *Journal of Geophysical Research*, Vol. 66, pp. 1865-1912, 1961.
14. Pekeris, C. L., Z. Alterman, and H. Jarosch, "Comparison of Theoretical with Observed Values of the Periods of the Free Oscillations of the Earth," *Proceedings of the National Academy of Sciences*, Vol. 47, pp. 91-98, 1961.
15. Kobayashi, N., and H. Takeuchi, "Surface Waves Propagating Along the Free Surface of a Semi-infinite Elastic Medium of Variable Density and Elasticity. (Part 5), Mantle Love Waves," *Geophysical Notes*, Tokyo University, Vol. 14, pp. 232-240, 1961.
16. Jobert, N., "Calcul de la Dispersion Des Ondes de Love de Grande Periode à la Surface de la Terre," *Annales de Géophysique* (Paris), Vol. 16, pp. 393-413, 1960.
17. Alterman, Z., H. Jarosch, and C. L. Pekeris, "Oscillations of the Earth," *Proceedings of the Royal Society (London)*, A, Vol. 252, pp. 80-95, 1959.
18. Love, A. E. H., *Some Problems of Geodynamics*, Cambridge University Press, Cambridge, England, 1911.
19. Hoskins, L. M., "The Strain of a Gravitating Sphere of Variable Density and Elasticity," *Transactions of the American Mathematical Society*, Vol. 21, pp. 1-43, 1920.
20. Jeans, J. H., "The Propagation of Earthquake Waves," *Proceedings of the Royal Society (London)*, A, Vol. 102, pp. 554-574, 1923.
21. Stoneley, R., "The Oscillations of the Earth," *Physics and Chemistry of the Earth*, Vol. 4, Pergamon Press, London, 1961.
22. Jobert, N., Evaluation de la Periode d'Oscillation d'Une Sphere Elastique Heterogene, Par Application du Principe de Rayleigh, *Comptes Rendus*, Vol. 243, pp. 1230-1232, 1956.
23. Carr, R., "Free Oscillations of a Gravitating Solid Sphere," Technical Report 32-164, Jet Propulsion Laboratory, Pasadena, 1961.
24. Carr, R., and R. L. Kovach, "Toroidal Oscillations of the Moon," *Icarus*, Vol. 1, pp. 75-76, 1962.
25. Takeuchi, H., M. Saito, and N. Kobayashi, "Free Oscillations of the Moon," *Journal of Geophysical Research*, Vol. 66, pp. 3895-3897, 1961.
26. Gutenberg, B., "The Asthenosphere Low Velocity Layer," *Annali di Geofisica* (Rome), Vol. 12, pp. 439-460, 1959.



- 
27. Birch, F., "Composition of the Earth's Mantle," *Geophysical Journal*, Vol. 4, pp. 295-311, 1961.
  28. Anderson, D. L., and D. Harkrider, "The Effect of Anisotropy on Continental and Oceanic Surface Wave Dispersion" (Abstr.), *Journal of Geophysical Research*, Vol. 67, p. 1627, 1962.
  29. Bolt, B., and A. Marussi, "Eigenvibrations of the Earth Observed at Trieste," *Geophysical Journal*, Vol. 6, pp. 299-311, 1962.
  30. Bath, M., and A. L. Arroyo, "Attenuation and Dispersion of G Waves," *Journal of Geophysical Research*, Vol. 67, pp. 1933-1942, 1962.
  31. Matumoto, T., and Y. Sato, "Phase Velocity of Long-Period Rayleigh and Love Waves as Observed in the Chilean Earthquake of May 22, 1960," presented orally at 43rd annual meeting American Geophysical Union, Washington, D. C.
  32. Brune, J., H. Benioff, and M. Ewing, "Long-Period Surface Waves from the Chilean Earthquake of May 22, 1960, Recorded on Linear Strain Seismographs," *Journal of Geophysical Research*, Vol. 66, pp. 2895-2910, 1961.
  33. Smith, S., "An Investigation of the Earth's Free Oscillations," Thesis, California Institute of Technology, 1961.